

## Interaction of the Lantibiotic Nisin with Mixed Lipid Bilayers: A $^{31}\text{P}$ and $^2\text{H}$ NMR Study<sup>†</sup>

Boyan B. Bonev,<sup>‡</sup> Weng C. Chan,<sup>§</sup> Barrie W. Bycroft,<sup>§</sup> Gordon C. K. Roberts,<sup>||</sup> and Anthony Watts<sup>\*,‡</sup>

*Biomembrane Structure Unit, Biochemistry Department, Oxford University, Oxford OX1 3QU, England,  
School of Pharmaceutical Sciences, University of Nottingham, Nottingham NG7 2RD, England,  
and Centre for Mechanisms of Human Toxicity, University of Leicester, Leicester LE1 9HN, England*

*Received January 20, 2000; Revised Manuscript Received June 26, 2000*

**ABSTRACT:** Nisin is a positively charged antibacterial peptide which binds to the negatively charged membranes of Gram-positive bacteria. The initial interaction of the peptide with model membranes of neutral (phosphatidylcholine) and negatively charged (phosphatidylcholine/phosphatidylglycerol) model lipid membranes was studied using nonperturbing solid state magic angle spinning (MAS)  $^{31}\text{P}$  NMR and  $^2\text{H}$  wide-line NMR. In the presence of nisin, the coexistence of two bilayer lipid environments was observed both in charged and in neutral membranes. One lipid environment was found to be associated with lipid directly interacting with nisin and one with noninteracting lipid. Solid state  $^{31}\text{P}$  MAS NMR results show that the acidic membrane lipid component partitions preferentially into the nisin-associated environment. Deuterium NMR ( $^2\text{H}$  NMR) of the selectively headgroup-labeled acidic lipid provides further evidence of a strong interaction between the charged lipid component and the peptide. The segregation of acidic lipid into the nisin-bound environment was quantified from  $^2\text{H}$  NMR measurements of selectively headgroup-deuterated neutral lipid. It is suggested that the observed lipid partitioning in the presence of nisin is driven, at least initially, by electrostatic interactions.  $^2\text{H}$  NMR measurements from chain-perdeuterated neutral lipids indicate that nisin perturbs the hydrophobic region of both charged and neutral bilayers.

The lipid membranes of cells are the sites of biological activity for many natural and synthetic cytolytic peptides. One particular class of peptides includes positively charged amphipathic molecules, which bind to negatively charged lipid membranes in a nonspecific way. This class includes a number of toxins and antibacterial peptides, which exercise their lytic action via the formation of nonselective transmembrane pores. Melittin (1–3) and magainin (4), for example, have been studied extensively and have become models for the design of a number of synthetic analogues, amphipathic in nature and positively charged, with enhanced cytolytic or bactericidal activity (5). It is currently accepted that the cytolytic action occurs in two steps, initial binding of the peptide to the target membrane governed by electrostatic attractive forces, followed by peptide oligomerization and then translocation across the membrane.

Nisin (Figure 1) is an amphipathic, positively charged peptide, produced by *Lactococcus lactis*, which is a member of the lantibiotic family of antimicrobial peptides (6); it inhibits the growth of a wide range of Gram-positive microorganisms and also inhibits the germination and/or outgrowth of spores of *Bacillus* and *Clostridium* species. It has been widely used as a preservative in the food industry

for a number of years (7, 8). The post-translational modification of the precursor peptide of nisin leads to the formation of dehydroalanine and dehydrobutyrine and, notably, of the thioether-bridged residues, lanthionine and methyllanthionine, which form five rings in the structure (6, 9, 10). The integrity of these rings is clearly important for the biological activities of nisin (11–13). There are two naturally occurring forms of nisin, nisin A and nisin Z, differing in only one residue (His or Asn at position 27) and with very similar bactericidal activities (14, 15).

In aqueous solution, nisin is very flexible, with no preferred overall conformation, although rings A and B, and particularly the linked rings D and E, clearly impose considerable local conformational constraints (6, 16, 17). When nisin is bound to detergent or lipid micelles (18) or lipid vesicles (19), its conformation becomes better defined. Under these circumstances, two structured regions have been identified: residues 3–19, containing rings A–C, and residues 22–28, containing rings D and E; these are flanked by flexible regions and linked by a “hinge” which may be important for insertion of the peptide into the lipid bilayer during pore formation (19).

The two actions of nisin and the related peptide subtilin, inhibition of bacterial growth and inhibition of the germination and/or outgrowth of spores, exhibit distinct structure–activity relationships, and must therefore involve different mechanisms (12, 20). Its bactericidal action appears to be due to the formation of pores in the bacterial membrane (6, 21). Model membrane studies show that nisin is active in

<sup>†</sup> The work was funded by the BBSRC (Grant 43/B04750 and a Senior Research Fellowship to A.W.), the EU (TMR, Contract FMRX-CT96-0004), and the HEFCE.

\* To whom correspondence should be addressed.

<sup>‡</sup> Oxford University.

<sup>§</sup> University of Nottingham.

<sup>||</sup> University of Leicester.

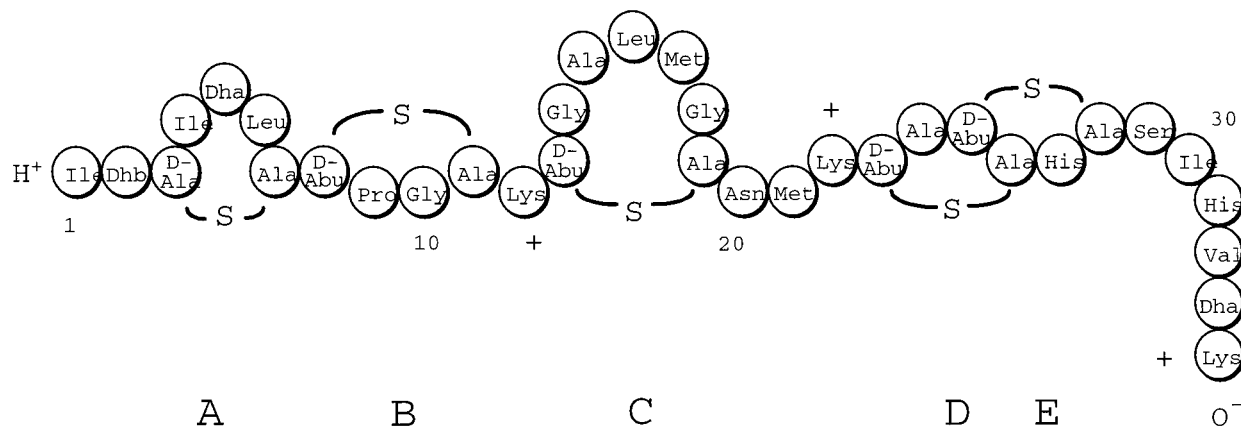


FIGURE 1: Primary sequence of nisin A. Dhb, dehydrobutyrine; Dha, dehydroalanine; D-Ala, alanine moiety of 3-methylanthionine; D-Abu,  $\alpha$ -aminobutyric acid moiety of 3-methylanthionine.

lipid vesicles (21–28), monolayers (29), and black lipid membranes (30, 31). In the absence of anionic phospholipids, nisin acts as an anion-selective carrier (21, 24, 28), but in the presence of anionic phospholipids, it forms nonselective, transient (lifetime on the order of milliseconds) pores in the target cytoplasmic membrane causing dissipation of the proton motive force ( $\Delta\Psi$ ) and efflux of ions, ATP, and other solutes vital to the microorganism (21, 23, 26, 28, 29). A transmembrane potential, inside negative, or a pH difference, cytoplasm alkaline, is needed for pore formation (21, 24, 26, 28, 32).

Nisin interacts more strongly with negatively charged than with neutral membranes (19, 22, 26, 27, 29, 30, 33, 34). When bound to SDS or DPC micelles, nisin is located within the headgroup region, rather than being inserted deeply into the micelle, with the hydrophobic residues in the structured regions (residues 3–19 and 22–28) facing into the micelle (18). Similarly in bilayers where  $\Delta\Psi = 0$ , there is evidence to indicate that nisin does not penetrate the lipid bilayer but rather binds to the headgroup region, in an orientation parallel to the plane of the bilayer (19, 22, 34). Several mutagenesis and fluorescence spectroscopic studies have led to differing conclusions regarding the importance of various parts of the nisin molecule for binding, and the depth of penetration into the bilayer (27, 29, 34); some of these differences may reflect the different phospholipid compositions of the bilayers or monolayers that are used.

Solid state NMR<sup>1</sup> is a direct and quantitative technique for investigating lipid–peptide and lipid–protein interactions in membranes. <sup>31</sup>P MAS NMR allows one to resolve the individual lipid components in the bilayer (35) and to measure changes in their isotropic chemical shift, CSA, and fwhh in response to modulation of the phosphate motions in the presence of proteins (35–37). Wide-line <sup>2</sup>H NMR provides a sensitive way to investigate the electrostatic environment of the lipid headgroups by measuring the changes in the quadrupole splittings of selectively deuterated lipids (38, 39). Incorporation of molecules in the bilayer

interior perturbs the order of the acyl chains. <sup>2</sup>H NMR of chain-perdeuterated lipids is sensitive to changes in the order at different methylene deuterium positions along the chains, and the quadrupole splitting

$$\Delta\nu_Q = \frac{3}{4}(e^2qQ/h)S_{CD}$$

from spectra of randomly oriented bilayers provides a measure of the deuterium order parameter  $S_{CD}$  (40). The quadrupole coupling constant ( $e^2qQ/h$ ) = 170 kHz (40, 41) for methylene C–D bonds.

In this paper, we describe the use of solid state NMR to investigate, in a direct and nonperturbing way, the interaction of nisin with lipid bilayers. Natural abundance <sup>31</sup>P magic angle spinning NMR and wide-line <sup>2</sup>H NMR of selectively headgroup-labeled lipids are used to probe the electrostatic interaction between nisin and the lipid headgroups, while <sup>2</sup>H NMR of chain-perdeuterated lipids provides information about the perturbation by nisin of the hydrophobic core of the lipid bilayer.

## MATERIALS AND METHODS

**Sample Preparation.** Synthetic unlabeled dimyristoylphosphatidylcholine (DMPC) and dimyristoylphosphatidylglycerol (DMPG) were purchased from Sigma and used without further purification. Headgroup-deuterated DMPC-*d*<sub>4</sub> was prepared from dimyristoylglycerol (Sigma) and deuterated ethanolamine (Merck) (42). Chain-perdeuterated DMPC was synthesized from perdeuterated myristic acid (43), by acylation of glycerophosphocholine (Sigma) (44). The final product was purified on a Silica Gel, mesh 60, liquid chromatography column and eluted with a 65/25/5 mixture of chloroform, methanol, and 28% ammonia. The lipid was found to migrate as a single spot on thin layer chromatography. Nisin was a gift of Aplin and Barrett and was used as supplied (98% pure).

For sample preparation, lipids were mixed in a chloroform/methanol (2/1) system. The solvent was removed under vacuum, and the lipid mixtures were dried under vacuum for 3–5 h. Nisin was added to the buffer [10 mM Tris, 10 mM NaCl, and 1 mM EDTA (pH 7.2) in <sup>2</sup>H-depleted water] at a concentration of 1 mg/mL. Nisin is soluble in water at this concentration at pH 7.2 (45). Approximately 20 mg of the lipid mixtures was hydrated in 10 mL of the

<sup>1</sup> Abbreviations: NMR, nuclear magnetic resonance; MAS, magic angle spinning; DMPC, 1,2-dimyristoylphosphatidylcholine; DMPC-*d*<sub>4</sub>,  $\alpha,\beta$ -[<sup>2</sup>H<sub>4</sub>]-1,2-dimyristoylphosphatidylcholine; DMPC-*d*<sub>54</sub>, 1,2-perdeuterodimyristoylphosphatidylcholine; DMPG, 1,2-dimyristoylphosphatidylglycerol; DMPG-*ds*,  $\alpha,\beta,\gamma$ -[<sup>2</sup>H<sub>3</sub>]-1,2-dimyristoylphosphatidylglycerol; fwhh, full width at half-height; MIC, minimal inhibitory concentration.

peptide-containing buffer. Each sample was subsequently put through five cycles of rapid freezing in liquid nitrogen and thawing at 50 °C. The MLV suspensions were then centrifuged (70 000 rpm, 1 h), and the pellet was loaded directly into 4 mm NMR zirconia rotors for the MAS experiments or 5 mm Pyrex NMR tubes for static wide-line measurements.

**NMR.**  $^{31}\text{P}$  and  $^2\text{H}$  NMR measurements were carried out on a CMX Infinity 500 spectrometer at a proton frequency of 500 MHz. A single  $90^\circ$  pulse was used for the acquisition of  $^{31}\text{P}$  spectra with broad-band decoupling at the proton frequency during acquisition. The  $90^\circ$  pulse length was 4  $\mu\text{s}$ , and the strength of the proton decoupling field was 20 kHz. The dwell time was 100  $\mu\text{s}$ , and 8192 points were collected in each experiment. Between 128 and 256 transients were averaged for each free induction decay (FID) with a 5 s delay between acquisitions.

Fast magic angle spinning (MAS) line shape analysis was performed by fitting simulated Lorentzian lines to the experimental spectra using Spinsight (Chemagnetics, Fort Collins, CO) and Felix (MSI, Cambridge, U.K.). The intensity of the individual lines was estimated from the integral of the simulated spectra. Analysis of the side-band patterns at a low spinning speed was performed by spectral simulation using an algorithm developed by Hertzfeld and Berger (46, 47). All  $^{31}\text{P}$  chemical shifts are measured relative to 0 ppm for 10% phosphoric acid.  $^2\text{H}$  powder line shapes were simulated using the GAMMA library (48) and a script developed by Glaubitz (49).

All  $^2\text{H}$  experiments were performed using a quadrupole echo sequence ( $90^\circ-\tau-90^\circ-\tau$  acquisition) (40, 41, 50) with a  $\tau$  of 40  $\mu\text{s}$ . The  $90^\circ$  pulse length was 4  $\mu\text{s}$ , and the repetition time was 0.5 s. Between 1024 and 96 000 transients were averaged per FID.

**Analysis.** In the analysis of DMPC/DMPG mixtures, the total fraction of DMPC,  $x_t$ , in the bilayer can be expressed in terms of its fractions in the nisin-free and nisin-associated environments,  $x_f$  and  $x_n$ , respectively, and the ratio between the two environments,  $R$ :

$$x_f R + x_n(1 - R) = x_t \quad (1)$$

where  $R (=s_f/s_n)$  is determined from the contribution from the nisin-free,  $s_f$ , and nisin-associated,  $s_n$ , environments to the NMR spectra. The DMPC fraction in the peptide-associated lipid is

$$x_n = (x_t - x_f R)/(1 - R) \quad (2)$$

The total fraction of DMPC in the mixed lipid bilayer  $x_t$  reflects the composition of the starting lipid mixture and is monitored by the relative spectral contribution from the lipid components in the  $^{31}\text{P}$  MAS NMR spectra and from the  $\alpha$ - and  $\beta$ -quadrupole splittings of headgroup-deuterated DMPC- $d_4$ . The composition of the fluid component is determined both from  $^{31}\text{P}$  MAS and from  $^2\text{H}$  wide-line NMR spectra (51).

## EXPERIMENTAL RESULTS

**Bilayer–Surface Interactions. (1) Phosphorus MAS NMR.** High-speed magic angle spinning  $^{31}\text{P}$  NMR was used to study the interaction of nisin A with model phospholipid bilayers.

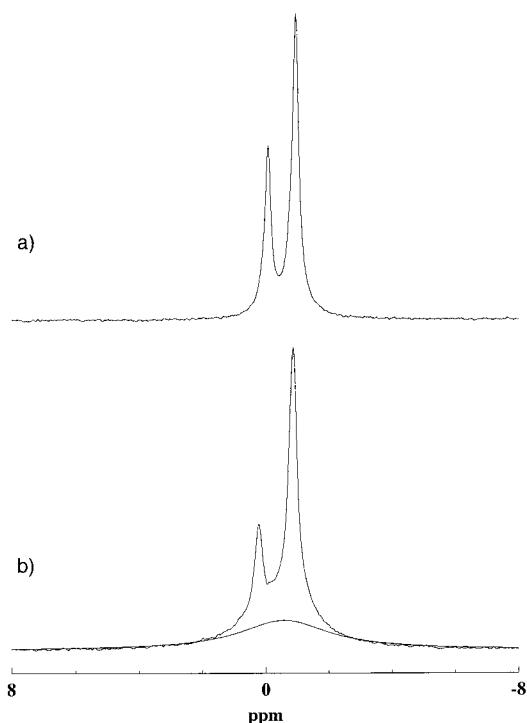


FIGURE 2:  $^{31}\text{P}$  MAS NMR spectrum of a mixture of DMPC and DMPG in a molar ratio of 2/1 (a) and in the presence of nisin A at a lipid-to-peptide molar ratio of 20 (b), with a spinning speed of 8 kHz at 30 °C. The simulated broad spectral component was obtained as described in the text. See Table 1 for spectral parameters.

Table 1:  $^{31}\text{P}$  Isotropic Chemical Shift ( $\sigma_i$ ), Line Width (fwhh), and Relative Intensity ( $I$ ) for DMPC and DMPG Phosphates without and with Nisin at a 1/20 Molar Ratio to the Total Amount of Lipid Determined from Spectra, Simulated To Fit the Experimental Spectra As Described in the Text<sup>a</sup>

	$\sigma_i$ (ppm)	fwhh (ppm)	$I$ (%)	$R$
<b>A</b>				
DMPC	-0.94	0.29	68	n/a
DMPG	-0.07	0.32	32	n/a
DMPC and nisin	-0.82	0.34	13	n/a
DMPG and nisin	0.27	0.33	37	n/a
broad resonance	-0.54	3.00	50	0.5
<b>B</b>				
DMPC	-0.91	0.36	n/d	n/a
DMPC and nisin	-0.88	0.39	n/d	n/a
broad resonance	-0.54	3.00	n/d	0.5

<sup>a</sup> The fraction of the nisin-free lipid component in the presence of nisin ( $R$ ) is shown for DMPC/DMPG (2/1 molar ratio) and for pure DMPC bilayers, DMPC/DMPG bilayers (A), and DMPC bilayers (B). Experimental conditions are described in the text. n/a, not defined. n/d, cannot be determined from the NMR spectra.

Two experimental systems were studied to monitor the interaction of nisin with charged bilayers, consisting of DMPC and DMPG, and with neutral bilayers of DMPC alone.

Figure 2a shows a  $^{31}\text{P}$  MAS NMR spectrum from a lipid bilayer composed of DMPC and DMPG in a 2/1 molar ratio at a spinning speed of 8 kHz. The resonance at -0.9 ppm arises from DMPC and that at 0.2 ppm from DMPG (Table 1). The spectrum can be simulated by a superposition of two Lorentzian lines with fwhhs of 0.32 and 0.29 ppm. The intensity of the DMPG resonance constitutes approximately 32% of the total spectral intensity, which reflects very well the fraction of DMPG in the mixture.

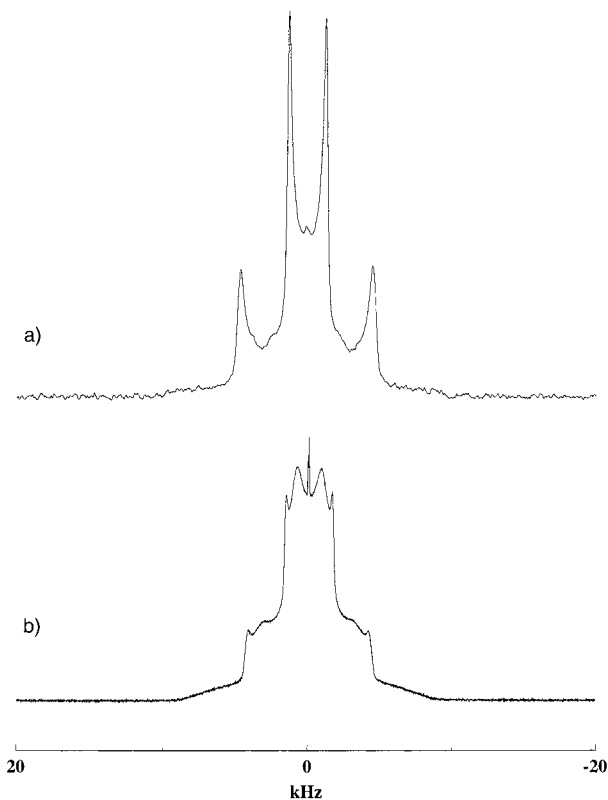


FIGURE 3:  $^2\text{H}$  NMR spectrum of a mixture of headgroup-deuterated DMPC- $d_4$  and DMPG in a molar ratio of 2/1 (a) and in the presence of nisin A at a lipid-to-peptide molar ratio of 20 (b), at 30 °C. See Table 2 for spectral parameters.

A spectrum from the same lipid mixture in the presence of nisin A in a lipid to peptide molar ratio of 20/1 is shown in Figure 2b. Two narrow resonances, as observed in the spectrum shown in Figure 2a, are still present. The fwhh of the DMPC resonance is 0.33 ppm and that of the DMPG resonance  $-0.34$  ppm. Spectral simulations require, in this case, the consideration of at least one additional resonance with a fwhh of 3.00 ppm, centered at approximately  $-0.54$  ppm. The similar values for the fwhh of the narrow resonances in the presence and in the absence of nisin suggest that the spectral intensity in the narrow spectral features originates from lipid not interacting with nisin. Such interpretation is further supported by the observation that the effective  $^{31}\text{P}$  chemical shift anisotropy of the narrow resonances, determined from slow (2 kHz) spinning speed MAS NMR, does not change upon addition of nisin (spectra not shown). While the origin of the broad spectral component is unknown, it is likely that it arises from an overlap of the spectral contributions from DMPC and DMPG interacting with membrane-associated nisin molecules. The observed line broadening reflects an enhanced phosphorus transverse relaxation rate, which may result from restrictions imposed on the motional freedom of the lipid headgroups during the interaction between the negatively charged lipid phosphates and the positively charged residues of nisin. The possibility that the broad spectral feature, also observed in  $^2\text{H}$  NMR spectra from labeled phospholipids, arises from an effective elevation of the main transition temperature of the lipid in the presence of nisin was ruled out after observing the persistence of the broad feature in  $^2\text{H}$  NMR spectra at temperatures exceeding 55 °C (cf. the inset of Figure 4).

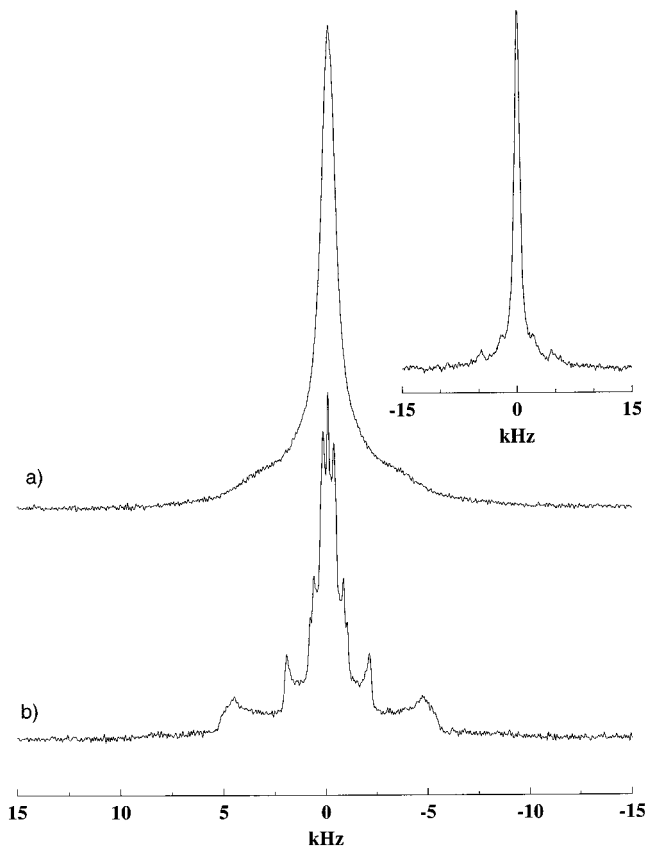


FIGURE 4:  $^2\text{H}$  NMR spectrum of a mixture of DMPC and headgroup deuterated DMPG- $d_5$  in a molar ratio of 2/1 (a) and in the presence of nisin A at a lipid-to-peptide molar ratio of 20 (b), at 30 °C. See Table 2 for spectral parameters. The inset shows the  $^2\text{H}$  NMR spectrum from the same bilayer in the presence of nisin at 55 °C.

The composition of the nisin-free phase in the presence of nisin can be determined from the relative intensity of each of the sharp DMPC and DMPG resonances with respect to one another, while the fraction of the fluid phase in the total bilayer lipid can be quantified from the cumulative intensity of both sharp features as a fraction of the total spectral intensity. The fraction of DMPG in the fluid phase, determined in this way, is 26%, and the fluid component in the spectrum is approximately 50% (Table 1).

The interaction of nisin with neutral lipid bilayers of DMPC was also investigated. A  $^{31}\text{P}$  MAS NMR spectrum of the DMPC MLV suspension (not shown) reveals a single resonance from DMPC with a fwhh of 0.36 ppm (Table 1). When nisin is added at a lipid/peptide molar ratio of 20/1, the spectrum becomes a superposition of a narrow component with a fwhh of 0.39 ppm (Table 1), and a broad component with a fwhh of 1.22 ppm (Table 1). It is suggested again that the broad resonance arises from nisin-associated lipid, while the narrow spectral component can be interpreted as the spectral contribution from nisin-free DMPC in the bilayer. The fraction of the nisin-free environment can be determined from spectral simulations to be approximately 50% (Table 1).

(2) *Deuterium NMR*. Wide-line  $^2\text{H}$  NMR of deuterated lipids is used to study the electrostatic interaction of nisin with the lipid headgroups and perturbations of the acyl chain motions. Headgroup-deuterated DMPC- $d_4$  is used as a nonperturbing probe of the interaction of nisin A with charged bilayers. The introduction of a relatively high



Table 2:  $^2\text{H}$  NMR Quadrupole Splittings Measured for DMPG Lipid Headgroup  $\alpha$ -,  $\beta$ -, and  $\gamma$ -Deuterons and DMPC Headgroup  $\alpha$ - and  $\beta$ -Deuterons in Bilayers Prior to (A) and Following the Addition of Nisin A (B)<sup>a</sup>

	$\alpha$ -splitting (kHz)	$\beta$ -splitting (kHz)	$\gamma$ -splitting (kHz)	<i>R</i>
<b>A</b>				
DMPC- <i>d</i> <sub>4</sub> /DMPG	9.2	2.7	n/a	n/a
DMPC/DMPG- <i>d</i> <sub>5</sub>	9.2	4.0	1.08	n/a
DMPC- <i>d</i> <sub>4</sub>	5.6*	6.1*	n/a	n/a
<b>B</b>				
DMPC- <i>d</i> <sub>4</sub> /DMPG and nisin	8.3	3.2	n/a	0.3/0.4
DMPC/DMPG- <i>d</i> <sub>5</sub> and nisin	n/d	n/d	n/d	n/d
DMPC- <i>d</i> <sub>4</sub> and nisin	5.5	5.5	n/a	0.5

<sup>a</sup> *R* is the fraction of the nisin-free lipid component in the presence of nisin. Experimental conditions are described in the text. \*, estimated extreme splittings from partially overlapping doublets. n/a, not defined. n/d, cannot be determined from the NMR spectra.

percentage (66.7%) of saturated chain neutral lipid into the negatively charged bilayer prevents the formation of non-lamellar phases, observed with pure DMPG under low-salt conditions (52) and in the presence of nisin (26). A  $^2\text{H}$  NMR spectrum from a mixture of DMPC-*d*<sub>4</sub> and DMPG in a 2/1 molar ratio is shown in Figure 3a. The spectrum consists of two overlapping Pake doublets, indicating rapid axially symmetric reorientation of lipid molecules in a liquid crystalline bilayer phase (40, 41). The most prominent spectral features are the sharp edges at  $\pm 4.6$  and  $\pm 1.3$  kHz arising, respectively, from the  $\alpha$ - and  $\beta$ -deuterons on the choline moiety of DMPC-*d*<sub>4</sub> molecules oriented at a 90° angle relative to the external magnetic field (Table 2). The observed deviation of the spectral intensity around the middle of the powder patterns from a spherically symmetric powder distribution results from a slight elongation of the liposomes in the high external magnetic field (53). The effective quadrupole splitting, used in the analysis, is unaffected by the vesicle deformation. The  $\alpha$ -splitting of the lipid mixture is 9.2 kHz, and the  $\beta$ -splitting is 2.7 kHz. These results agree with previous measurements from DMPC/DMPG mixtures of the same composition by Marassi and Macdonald (54) and Sixl and Watts (42).

Figure 3b shows a  $^2\text{H}$  NMR spectrum from a 2/1 DMPC-*d*<sub>4</sub>/DMPG mixture where nisin was added at a lipid/peptide molar ratio of 20/1. Two components can be resolved in the spectrum arising from the sharp 90° edges of two Pake doublets at 8.3 and 3.2 kHz ( $\alpha$ - and  $\beta$ -splittings, respectively) and a broad spectral feature, arising from a bilayer lipid environment with a reduced symmetry of molecular motions. The latter, observed as the spectral intensity between the  $\alpha$ - and  $\beta$ -splittings of DMPC-*d*<sub>4</sub> and in the region around  $\pm 1$  kHz, arises from a spectral distribution very different from the Pake distribution and cannot be interpreted in terms of contributions from individual deuterons. It is suggested that it arises from lipids associated with membrane-bound nisin. The Pake doublets suggest the presence of bilayer lipid in the liquid crystalline phase which does not have an immediate interaction with nisin. It is likely that the two lipid environments correspond to lateral bilayer phases, coexisting within the same bilayer in thermodynamic equilibrium.

The effect of nisin A on charged lipid bilayers can be investigated further by labeling specifically the headgroup of the charged lipid component DMPG-*d*<sub>5</sub>. The  $^2\text{H}$  NMR spectrum of a mixture of DMPC and DMPG-*d*<sub>5</sub> in a 2/1

molar ratio is shown in Figure 4a. The spectrum consists of superimposed powder [Pake (55)] doublets, arising from deuterons at the  $\alpha$ -,  $\beta$ -, and  $\gamma$ -positions on the phosphatidylglycerol moiety. The  $\alpha$ -,  $\beta$ -, and  $\gamma$ -doublets appear in decreasing order of their effective quadrupole splitting (56), which are, respectively, 9.2, 4.0, and 1.08 kHz. The splitting at approximately 1.4 kHz arises from the  $\beta$ -deuteron of D-glycerol, present in the racemic mixture used in DMPG-*d*<sub>5</sub> synthesis. The spectrum in Figure 4a arises from deuterons undergoing a fast, axially symmetric motion, characteristic of lipids in a liquid crystalline bilayer (42). A low-intensity doublet appears at approximately 2 kHz.

Addition of nisin at a lipid/peptide molar ratio of 20/1 results in a reduction in the motional symmetry of the DMPG-*d*<sub>5</sub> molecules (Figure 4b). The main spectral features of the new lipid state resemble those expected for a finite number of restricted jumps between different sites for the lipid headgroup (57–59). Such a reduction in the symmetry of headgroup motions suggests that in the presence of nisin the headgroup dynamics approaches the intermediate regime. The overall spectral width remains practically unchanged, which may suggest some disordering effect of nisin on the lipid headgroups. The more pronounced changes in the spectral intensity distribution on DMPG than on DMPC headgroups in the presence of nisin reflect the presence of a preferential interaction between the peptide and the charged lipid component.

The spectral feature arising from motionally restricted DMPG-*d*<sub>5</sub> persists at temperatures exceeding 55 °C (see the inset of Figure 4). Therefore, this phase emerges as a result of nisin–lipid interactions, which are stronger than the lipid–lipid interactions in a lipid gel phase. At 55 °C, the motionally restricted phase is in equilibrium with a lipid population in the liquid crystalline phase. The slight elevation in *T*<sub>m</sub> of the nisin-free lateral phase results from the use of racemic glycerol during DMPG-*d*<sub>5</sub> synthesis and, possibly, from a slight variation in the residual salt content (see the Discussion).

Headgroup-labeled DMPC-*d*<sub>4</sub> is used to examine the interaction of nisin A with neutral lipid bilayers (spectra not shown). At 30 °C, the spectrum is characteristic of fast axially symmetric lipid motions and suggests that DMPC-*d*<sub>4</sub> is in a liquid crystalline phase. At this temperature, the  $\beta$ -deuteron quadrupole splitting almost completely overlaps the  $\alpha$ -splitting (51, 60). Both splittings are between 5.6 and 6.1 kHz. Addition of nisin to the DMPC-*d*<sub>4</sub> suspension at a lipid/peptide molar ratio of 20/1 results in a  $^2\text{H}$  NMR spectrum which is a superposition of two components, one characteristic of a liquid crystalline phase and another suggesting the presence of a lipid population with restricted molecular motions. The quadrupole splitting of the spectral component from the liquid crystalline phase for both labeled positions is equal to 5.5 kHz. The slight difference between the  $\alpha$ - and  $\beta$ -quadrupole splitting, observed in the form of a small shoulder on the outer side of the 90° edges of the pure lipid powder spectrum, is no longer observed. A comparison of the quadrupole splittings of DMPC-*d*<sub>4</sub> alone and in the presence of nisin reveals a very weak response of the lipid headgroups to the presence of the peptide. Due to the similar values of the  $\alpha$ - and  $\beta$ -quadrupole splittings for the peptide-free bilayer, the electrostatic interaction between nisin A and

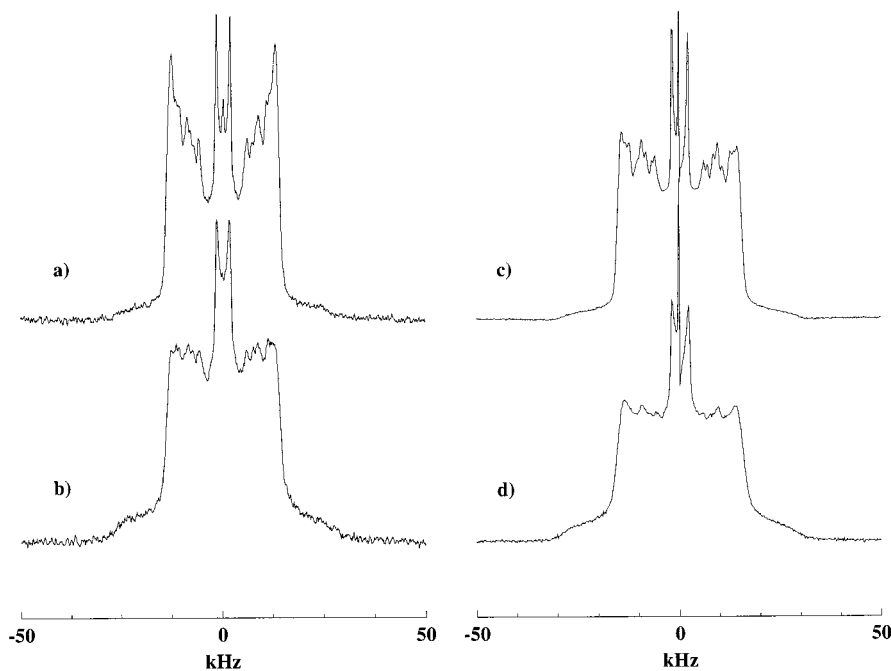


FIGURE 5:  $^2\text{H}$  NMR spectra of chain-perdeuterated DMPC- $d_{54}$  at 30 °C in a mixture with DMPG at a molar ratio of 2/1 (a), the same mixture in the presence of nisin A at a lipid-to-peptide molar ratio of 20 (b), in pure bilayers (c), and in pure bilayers with nisin A at a lipid-to-peptide molar ratio of 20 (d).

the zwitterionic lipid component cannot be quantified at 30 °C.

**Nisin–Bilayer Core Interactions.** Chain-perdeuterated DMPC- $d_{54}$  was used to study the response of the hydrocarbon chain region of the lipid bilayer to addition of nisin in the presence and in the absence of a charged lipid component. A  $^2\text{H}$  NMR spectrum from a DMPC- $d_{54}$ /DMPG mixture in a molar ratio of 2/1 is shown in Figure 5a. The spectrum is a superposition of powder doublets, which indicates that the lipid chains undergo axially symmetric motions in a fluid phase. The maximum observed quadrupole splittings of about 26 kHz arise from the almost overlapping  $90^\circ$  edges of deuterons at methylene positions 2–7, close to the glycerol backbone (40). The smaller resolved quadrupole splittings between 25 and 15 kHz arise from methylene deuterons between the middle of the chain and the terminal methyl groups (methylene positions 7–13). The chain methyl groups give rise to the distinct powder doublet with the smallest splitting of 3.0 kHz. The quadrupole splittings of the chain deuterons in the liquid crystalline phase are sensitive to changes in chain segmental motions and can be used as a measure of the order along the lipid acyl chains (40, 41). The spectrum of Figure 5a exhibits a small deviation from a Pake line shape, which indicates a slight elongation of the charged phospholipid vesicles in the external magnetic field (53). These spectral changes affect the distribution of spectral intensity but not the effective deuterium quadrupole splittings.

After addition of nisin to the DMPC- $d_{54}$ /DMPG bilayer at a lipid to peptide molar ratio of 20/1, the  $^2\text{H}$  NMR spectrum from DMPC- $d_{54}$  shows that the bilayer is still in the liquid crystalline state (Figure 5b). The maximum spectral width remains unchanged. A slight redistribution of spectral intensity at close to maximum splitting is observed while the methyl splittings remain unchanged. The enhancement of the  $90^\circ$  edges, observed in the absence of nisin, is no longer present, possibly because of the reduced net charge

in the peptide-containing bilayers and a consequent reduction in vesicle ellipticity.

The effect of nisin on the hydrophobic region of pure DMPC- $d_{54}$  bilayers was also examined using  $^2\text{H}$  NMR. The pure DMPC- $d_{54}$  bilayer is in the liquid crystalline state, and the spectrum is a superposition of Pake doublets (Figure 5c) with a maximum quadrupole splitting of approximately 28 kHz. Addition of nisin results in a spectrum with an essentially unchanged overall width (Figure 5d). The resolution of most  $90^\circ$  singularities, however, is lost. The deuterium lines are broadened, and only major groups of methylenes with similar order parameters, giving rise to splittings of approximately 27, 18, and 11 kHz, can be resolved. One possible explanation for the observed line broadening is that the presence of nisin might enhance the transverse relaxation rate of the chain deuterons. Such enhancement, if present, does not appear to have a differential effect on deuterons at different positions along the acyl chain. Another change in the spectral intensity distribution is a small reduction at close to minimum methylene splitting, observed after nisin is added. An increase in spectral intensity in the regions between  $-28$  and  $-15$  kHz and between 15 and 28 kHz indicates diminished vesicle ellipticity in the presence of nisin, presumably in response to a reduction in the bilayer net surface charge density. Further analysis of the methylene deuterium spectra by means of de-Pake-ing would be unreliable due to vesicle elongation in the presence of a charged lipid without nisin and due to loss of spectral resolution from neutral bilayers in the presence of nisin.

**Quantification of the Stoichiometries of Nisin–Lipid Interactions.** The relative intensities of  $^{31}\text{P}$  NMR lines were used to quantify the fraction of DMPC in the negatively charged DMPC/DMPG lipid bilayers before and after nisin was added. The initial fraction of DMPC in the bilayer, determined in this way, is 0.68 ( $x_i$ ) (Table 3). The DMPC fraction in the nisin-free bilayer is 0.74 ( $x_i$ ), and the

Table 3: Calculated DMPC Molar Fraction in the Pure Lipid Bilayer ( $x_t$ ) and after Addition of Nisin in the Nisin-Free ( $x_f$ ) and Nisin-Associated ( $x_n$ ) (peptide/lipid ratio of 1/20) Lipid Environment

DMPC fraction	$x_t$	$x_f$	$x_n$
from $^{31}\text{P}$ MAS	0.68	0.74	0.62
from $^2\text{H}$	0.67	0.80	0.58/0.61
per 20 lipid molecules	13.3	16	11.6/12.2

contribution from the nisin-free spectral components is 0.50 ( $R$ ). The DMPC fraction in the nisin-associated environment can be calculated using eq 2 to be  $\approx 0.62$  ( $x_n$ ). This corresponds to 12.4 DMPC molecules in 20 lipid molecules.

The partitioning of DMPC and DMPG between the nisin-free and nisin-associated environment can be quantified using  $^2\text{H}$  NMR, as well. The relative magnitude of the  $\alpha$ - and  $\beta$ -quadrupole splittings can be used to measure the surface charge in the bilayer headgroup region (38, 39). In particular, a reduction in the  $\alpha$ -splitting and an increase in the  $\beta$ -splitting indicate a change in the surface charge to more positive values (38). A change in the lipid order, in contrast, would be accompanied by a change of both splittings in the same direction. Therefore, the observed increase in the choline  $\beta$ -splitting and a decrease in the  $\alpha$ -splitting are a good indication that the interaction between nisin and the DMPC/DMPG bilayer is of electrostatic nature. The observed changes in the values of the DMPC- $d_4$   $\alpha$ - and  $\beta$ -quadrupole splittings in the DMPC- $d_4$ /DMPG mixture upon addition of nisin are compared to the quadrupole splittings from a series of DMPC- $d_4$ /DMPG mixtures, measured by Marassi and Macdonald (54). The fraction of DMPC- $d_4$  in the nisin-free bilayer can be obtained from  $^2\text{H}$  NMR data or in a simple way from the  $^{31}\text{P}$  NMR measurements. At the same time, the spectrum of the nisin-associated bilayer environment cannot be used directly to determine its composition. This can be done by using the already determined composition of the fluid phase and its fraction in the bilayer. A spectral subtraction method, similar to the method used by Morrow et al. (61) and Huschilt et al. (62), is used to determine the contribution of the fluid component in the spectrum of Figure 3b. Two Pake doublets are simulated with quadrupole splittings matching the ones measured from the spectrum in Figure 3b. The simulated and experimental spectra are then normalized to the same intensity,  $M_0$ , assuming that the transverse relaxation rates for the deuterons in the two phases are similar. The  $90^\circ$  edges of the experimental  $\alpha$ -splitting are found to be canceled out by subtraction of 30–40% of the simulated spectrum from the spectrum in Figure 3b. The  $90^\circ$  edges of the  $\beta$ -splittings are used as a supplementary criterion only, since the ellipticity of the MLV, producing distortions on the experimental  $\alpha$ -doublets in the presence of nisin, cannot be estimated. Using the values of  $x_t$  (0.67) and  $x_f$  (0.80), determined earlier, the calculated DMPC fraction in the nisin-associated bilayer is 0.58 and 0.61 ( $x_n$ ) when  $R = 0.30$  and  $0.40$ , respectively. Since the nisin-to-lipid ratio is 1/20 in this experiment, these values correspond to 11.6 and 12.2 DMPC molecules per 20 lipid molecules. The DMPC fraction in the bilayer prior to addition of nisin has 13.3 molecules in 20 molecules, and in the nisin-free bilayer phase in the presence of nisin, there are 16 DMPC molecules in every 20. The withdrawal of acidic lipid into peptide-associated domains is similar to the segregation of phosphatidylglycerol by a charged peptide, derived from the

C-terminus of HIV-1 glycoprotein gp160, observed by Gawrsich et al. (63).

When nisin interacts with neutral bilayers, the spectral fraction of the nisin-free lipid component in the DMPC- $d_4$ /nisin bilayer is determined from  $^2\text{H}$  NMR spectra by the spectral subtraction method. The contribution from the fluid spectral component is approximately 50% (Table 2), which agrees with the  $^{31}\text{P}$  MAS NMR results (Table 1).

## DISCUSSION

The observations of (i) the decrease in the  $^{31}\text{P}$  NMR spectral intensity of the DMPG resonance relative to that of DMPC in the nisin-free bilayer upon addition of nisin, (ii) the reduction in the net charge in the fluid lipid environment, measured by  $^2\text{H}$  NMR of headgroup-labeled DMPC- $d_4$ , and (iii) the strong effect of nisin on labeled DMPG- $d_5$  headgroup dynamics all provide strong and direct evidence that nisin interacts preferentially with the charged bilayer lipid component. The larger fraction of nisin-associated lipids in charged bilayers compared to neutral bilayers (Table 2B) indicates a higher affinity of nisin for membranes containing charged lipids.

The isotropic chemical shifts of both DMPC and DMPG phosphates in the lipid mixture undergo a slight upfield shift upon addition of nisin (see Table 1A). A similar lower-magnitude nisin-induced upfield shift is observed in the chemical shift of pure DMPC bilayers. Such changes reflect changes in the electrostatic environment of the lipid phosphates upon addition of nisin.

The relatively weak electrostatic perturbation of the DMPC- $d_4$  headgroups in neutral bilayers by nisin in comparison to charged bilayers reflects an increased distance in the former case between the nisin charges and the lipid headgroup dipole. Since nisin has been shown to have a similar orientation in charged and neutral bilayers (34), the observed changes may arise from differences in penetration depth of nisin into the two lipid bilayers.

A broad feature, characteristic of a lipid environment with restricted motional freedom, is observed in the  $^{31}\text{P}$  and  $^2\text{H}$  NMR spectra from lipid headgroups in the presence of nisin. One possibility is that this motionally restricted lipid environment may reflect the formation of lipid gel phase domains as a result of the reduction of the bilayer surface charge in the vicinity of the positively charged nisin molecules in a way, similar to the elevation of the main transition temperature of DMPG at low pH (64, 65). However, the overall width of the observed  $^2\text{H}$  NMR line, arising from this environment, is smaller than the expected width of a gel phase spectrum. Also, changes in the DMPG headgroup charge are not expected to produce elevation of the lipid  $T_m$  above  $42^\circ\text{C}$ . In our experiments, the broad feature is observed in  $^2\text{H}$  NMR spectra from DMPC- $d_4$  and DMPG- $d_5$  at temperatures exceeding  $55^\circ\text{C}$  (e.g., as in the inset of Figure 4). Therefore, the broad spectral feature is not a lipid gel phase but rather a lipid environment dominated by nisin–lipid interactions that are stronger than the lipid–lipid interactions resulting in the formation of gel phases.

Additional investigation into the origin of the broad spectral component, observed in the  $^{31}\text{P}$  spectra of phospholipids in the presence of nisin, is required before it can be used in a quantitative way to elucidate the phase behavior



of lipid bilayers. While the composition of the nisin-free environment can be quantified with an accuracy better than  $\pm 5\%$ , modeling of the broad spectral component is more sensitive to spectral manipulations, such as phase and baseline corrections. This, presumably, is due to the fact that the broad resonance is a superposition of two lines. As a result, the uncertainty in the less mobile fraction determination from high-speed  $^{31}\text{P}$  MAS NMR may be much greater than stated. The relative fraction of DMPG in the nisin-free component decreases with increasing amounts of added nisin and can be quantified with accuracy. At the same time, the spectral contribution of the putatively nisin-associated lipid displays changes, upon cumulative addition of nisin, which are on the same order as the expected overall change in the intensity of this spectral component. This has necessitated the use of  $^2\text{H}$  NMR from selectively labeled lipids to obtain the spectral fraction from the nisin-associated component in a more reliable way.

One additional point needs clarification in view of the proposed two-dimensional segregation of the charged membrane lipid by nisin. The  $^2\text{H}$  NMR spectrum of DMPG- $d_5$  at 30 °C (Figure 4b), unlike the spectrum of DMPC- $d_4$  in the DMPC/DMPG mixture, gives no indication of coexistence of a nisin-associated lipid environment with restricted headgroup motions and a lipid phase with axial symmetric headgroup deuteron dynamics at this temperature. However, the occurrence of a fluid phase in the DMPC/DMPG- $d_5$  mixture in the presence of nisin A is observed when the temperature is elevated to 50 °C (inset of Figure 4). The coexistence of the two lipid environments can also be converted into a single, motionally restricted lipid environment with spectral features similar to those observed in Figure 4b, when the ionic strength of the aqueous phase is increased to 100 mM NaCl (spectrum not shown). The differences in the lateral phase behavior of the DMPG- $d_5$ -containing system and the other DMPG-containing bilayers might be attributed to some additional heterogeneity introduced into the system by the presence of equimolar amounts of both headgroup glycerol enantiomers. In addition, as a result of the sensitivity of the system to ionic strength, the differences, observed between the phase behavior of the DMPC- $d_4$  and DMPG- $d_5$ -containing mixtures, may reflect the presence of trace amounts of salts in the preparation of DMPG- $d_5$ .

$^{31}\text{P}$  MAS from the phospholipid bilayers and wide-line  $^2\text{H}$  NMR measurement from bilayers of headgroup-labeled DMPC, with and without negatively charged lipid component DMPG, reveal the coexistence of at least two bilayer environments in the presence of nisin. The spectral intensity distribution in  $^2\text{H}$  NMR line shapes and the overall magnitude of the quadrupole splittings in both coexisting lipid environments demonstrates that all lipid in the system is in a bilayer phase. It is suggested that the two lipid environments observed in the presence of nisin coexist laterally within the same lipid bilayer. The rate of exchange of lipids between the two environments is governed by the strength of the lipid-peptide interaction. The observed superposition of spectra, rather than an average spectrum from the two lipid environments, suggests that the rate of exchange is slower than the inverse time scale of the  $^2\text{H}$  NMR experiment ( $\sim 10^3$  Hz) [cf. Bloom and Thewalt (66)]. The border between two lateral lipid environments creates a local weaknesses in the

bilayer (67), which may be implicated in peptide translocation during pore formation or in anion transport.

The highly fluid nisin-free lipid environment can be visualized as a matrix in which islands of nisin with associated lipid float at much reduced mobility. In this context, the nisin-free environment can be characterized as a large ensemble of molecules representing a true lateral phase. In the nisin-associated lipid, on the other hand, a large number of molecules determine the average behavior seen in the NMR experiment without necessarily allowing for a direct lipid exchange to occur between lipid associated with different nisin molecules. The number of lipid molecules in each nisin-associated cluster may be small; therefore, the nisin-associated phase is not a true thermodynamic phase. The reduction in membrane fluidity, observed by Kordel et al. (22) and Giffard et al. (30), upon addition of nisin to bilayers can be explained either by assuming the formation of small lipid aggregates, associated with single peptide molecules, or by considering large lipid-peptide domains of macroscopic size. In the former case, the effective molecular mass of a complex of nisin and associated lipids would result in a much lower effective lateral mobility in the membrane, while in the latter, the reduced mobility within a motionally restricted phase would be detected.

Nisin appears to interact more strongly with bilayers composed of lipids with acidic headgroups than with bilayers composed of neutral lipids. This description of the state of the lipid bilayer prior to permeabilization is important for understanding the mechanism of action of nisin. The translocation of anionic molecules across neutral bilayers in the presence of nisin can occur when the positively charged molecules of nisin, immersed in the hydrophobic region of the PC bilayer, interact with the negatively charged molecule on the opposite side of the membrane. The potentially neutral complex, formed in this way, may be entropically driven to either side of the bilayer across mismatched bilayer regions between nisin-associated and nisin-free lipids. In the presence of negatively charged lipid in the membrane, a strong electrostatic interaction leads to a surface localization of nisin. A substantial electromotive force would be necessary, for example, in the form of a transmembrane potential difference, to overcome the strong electrostatic interaction between nisin and the anionic lipid headgroups. In this case, it is possible that the more energetically favorable structure is a transmembrane oligomer, rather than a nisin-anion transmembrane complex.

## ACKNOWLEDGMENT

We are indebted to Aplin and Barrett for the donation of nisin, to Peter Fisher for the synthesis of the headgroup-deuterated phospholipids, to Eefjan Breukink for the critical discussion of the manuscript, and to Clemens Glaubitz for the help with the powder spectra simulation software.

## REFERENCES

1. Dufourcq, J., Faucon, J.-F., Fourche, G., Dasseux, J.-L., Le Maire, M., and Gulik-Krzywicki, T. (1989) *Biochim. Biophys. Acta* 859, 33–48.
2. Dempsey, C. E., and Watts, A. (1987) *Biochemistry* 26, 5803–5811.



3. Beschiaschvili, G., and Seelig, J. (1990) *Biochemistry* 29, 52–58.
4. Matsuzaki, K. (1998) *Biochim. Biophys. Acta* 1376, 391–400.
5. Hirsh, D. J., Hammer, J., Maloy, W. L., Blazyk, J., and Schaefer, J. (1996) *Biochemistry* 35, 12733–12741.
6. Sahl, H. G., Jack, R. W., and Bierbaum, G. (1995) *Eur. J. Biochem.* 230, 827–853.
7. Rayman, K., and Hurst, A. (1984) in *Biotechnology of Industrial Antibiotics* (Vandamme, E. J., Ed.) pp 607–628, Dekker, New York.
8. Delves-Broughton, J., Blackburn, P., Evans, R. J., and Hugenholtz, J. (1996) *Antonie van Leeuwenhoek* 69, 193–202.
9. Gross, E., and Morrell, J. L. (1971) *J. Am. Chem. Soc.* 93, 4634–4635.
10. Chan, W. C., Lian, L. Y., Bycroft, B. W., and Roberts, G. C. K. (1989) *J. Chem. Soc., Perkin Trans. 1*, 2359–2367.
11. Chan, W. C., Bycroft, B. W., Lian, L. Y., and Roberts, G. C. K. (1989) *FEBS Lett.* 300, 56–62.
12. Chan, W. C., Dodd, H. M., Horn, N., Maclean, K., Lian, L.-Y., Bycroft, B. W., Gasson, M. J., and Roberts, G. C. K. (1996) *Appl. Environ. Microbiol.* 62, 2966–2969.
13. Chan, W. C., Leyland, M., Clark, J., Dodd, H. M., Lian, L.-Y., Gasson, M. J., Bycroft, B. W., and Roberts, G. C. K. (1996) *FEBS Lett.* 390, 129–132.
14. Mulders, J. W. M., Boerrigter, I. J., Rollema, H. S., Siezen, R. J., and de Vos, W. M. (1991) *Eur. J. Biochem.* 201, 581–584.
15. De Vos, W. M., Mulders, J. W. M., Siezen, R. J., Hugenholtz, J., and Kuipers, O. P. (1993) *Appl. Environ. Microbiol.* 59, 213–218.
16. Lian, L. Y., Chan, W. C., Morley, S. D., Roberts, G. C. K., Bycroft, B. W., and Jackson, D. (1992) *Biochem. J.* 283, 413–420.
17. van de Ven, F. J. M., Van den Hooven, H. W., Konings, R. N. H., and Hilbers, C. W. (1991) *Eur. J. Biochem.* 202, 1181–1188.
18. van den Hooven, H. W., Spronk, C. A. E. M., van de Kamp, M., Konings, R. N. H., Hilbers, C. W., and van de Ven, F. J. M. (1996) *Eur. J. Biochem.* 235, 394–403.
19. El-Jasmiti, R., and Lafleur, M. (1997) *Biochim. Biophys. Acta* 1324, 151–158.
20. Liu, W., and Hansen, J. N. (1993) *Appl. Environ. Microbiol.* 59, 648–651.
21. Moll, G. N., Roberts, G. C. K., Konings, W. N., and Driessen, A. J. M. (1996) *Antonie van Leeuwenhoek* 69, 185–191.
22. Kordel, M., Schüller, F., and Sahl, H.-G. (1989) *FEBS Lett.* 244, 99–102.
23. Gao, F. H., Abee, T., and Konings, W. N. (1991) *Appl. Environ. Biol.* 57, 2164–2170.
24. Garcerá, M. J. G., Elferink, M. G. L., Driessen, A. J. M., and Konings, W. N. (1993) *Eur. J. Biochem.* 212, 417–422.
25. Abee, T. (1995) *FEMS Microbiol. Lett.* 129, 1–10.
26. Driessen, A. J. M., van den Hooven, H. W., Kuiper, W., van de Kamp, M., Sahl, H.-G., Konings, R. N. H., and Konings, W. N. (1995) *Biochemistry* 34, 1606–1614.
27. Martin, I., Ruysschaert, J.-M., Sanders, D., and Giffard, C. J. (1996) *Eur. J. Biochem.* 239, 156–164.
28. Moll, G. N., Clark, J., Chan, W. C., Bycroft, B. W., Roberts, G. C. K., Konings, W. N., and Driessen, A. J. M. (1997) *J. Bacteriol.* 179, 135–140.
29. Demel, R. A., Peelen, T., Siezen, R. J., de Kruijff, B., and Kuipers, O. P. (1996) *Eur. J. Biochem.* 235, 267–274.
30. Giffard, C. J., Ladha, S., Mackie, A. R., Clark, D. C., and Sanders, D. (1996) *J. Membr. Biol.* 151, 293–300.
31. Palmeri, A., Pepe, I. M., and Rolandi, R. (1996) *Thin Solid Films* 284–285, 822–824.
32. Sahl, H. G., Kordel, M., and Benz, R. (1987) *Arch. Microbiol.* 149, 120–124.
33. Breukink, E., van Kraaij, C., Demel, R. A., Siezen, R. J., Kuipers, O. P., and de Kruijff, B. (1997) *Biochemistry* 36, 6968–6976.
34. Breukink, E., van Kraaij, C., van Dalen, A., Demel, R. A., Siezen, R. J., de Kruijff, B., and Kuipers, O. P. (1998) *Biochemistry* 37, 8153–8162.
35. Pinheiro, T. J. T., and Watts, A. (1994) *Biochemistry* 33, 2459.
36. Spooner, P. J. R., and Watts, A. (1992) *Biochemistry* 31, 10129–10138.
37. Carbone, M. A., and Macdonald, P. M. (1996) *Biochemistry* 35, 3368–3378.
38. Akutsu, H., and Seelig, J. (1981) *Biochemistry* 20, 7366–7373.
39. Seelig, J., Macdonald, P. M., and Scherer, P. G. (1987) *Biochemistry* 26, 7535–7541.
40. Seelig, J. (1977) *Q. Rev. Biophys.* 10, 353–418.
41. Davis, J. H. (1983) *Biochim. Biophys. Acta* 737, 117.
42. Sixl, F., and Watts, A. (1983) *Proc. Natl. Acad. Sci. U.S.A.* 80, 1613–1615.
43. Hsiao, C. Y. Y., Ottaway, C. A., and Wetlaufer, D. B. (1980) *Lipids* 9, 813.
44. Gupta, C. M., Rahakrishnan, R., and Khorana, H. G. (1977) *Proc. Natl. Acad. Sci. U.S.A.* 74, 4315.
45. Rollema, H. S., Kuipers, O. P., Both, P., de Vos, W. M., and Siezen, R. J. (1997) *Eur. J. Biochem.* 247, 114–120.
46. Herzfeld, J., and Berger, A. E. (1980) *J. Chem. Phys.* 73, 6021.
47. de Groot, H. J. M., Smith, S. O., Kolbert, A. C., Courtin, J. M. L., Winkel, C., Lugtenbourg, J., Herzfeld, J., and Griffin, R. G. (1991) *J. Magn. Reson.* 91, 30–38.
48. Smith, S. A., Levante, T. O., Meier, B. H., and Ernst, R. R. (1994) *J. Magn. Reson., Ser. A* 106, 75.
49. Glaubitz, C. (1998) D.Philos. Thesis, University of Oxford, Oxford, England.
50. Davis, J. H., Jeffrey, K. R., Bloom, M., Valic, M. I., and Higgs, T. P. (1976) *Chem. Phys. Lett.* 42, 390.
51. Marassi, F. M., and Macdonald, P. M. (1992) *Biochemistry* 31, 10031–10036.
52. Heimburg, T., and Biltonen, R. L. (1994) *Biochemistry* 33, 9477–9488.
53. Brumm, T., Möps, A., Dolainsky, C., and Bayerl, T. (1992) *Biophys. J.* 61, 1018–1024.
54. Marassi, F. M., and Macdonald, P. M. (1991) *Biochemistry* 30, 10558–10566.
55. Sternin, E., Bloom, M., and MacKay, A. L. (1983) *J. Magn. Reson.* 55, 274.
56. Wohlgemuth, R., Waespe-Šarčević, N., and Seelig, J. (1980) *Biochemistry* 19, 3315–3321.
57. Spooner, P. J. R., Duralski, A. A., Rankin, S. E., Pinheiro, T. J. T., and Watts, A. (1992) *Biophys. J.* 65, 106–112.
58. Spiess, H. W., and Silescu, H. (1981) *J. Magn. Reson.* 42, 381–389.
59. Wittebort, R. J., Olejniczak, E. T., and Griffin, R. G. (1987) *J. Chem. Phys.* 86, 5411–5420.
60. Bonev, B. B., and Morrow, M. R. (1995) *Biophys. J.* 69, 518–523.
61. Morrow, M. R., Huschilt, J. C., and Davis, J. H. (1985) *Biochemistry* 24, 5396–5406.
62. Huschilt, J. C., Hodges, R. S., and Davis, J. H. (1985) *Biochemistry* 24, 1377–1386.
63. Gawrsh, K., Barry, J. A., Holte, L. L., Sinnwell, T., Bergelson, L. D., and Ferretti, J. A. (1995) *Mol. Membr. Biol.* 12, 83–88.
64. Cevc, G., Seddon, J. M., and Marsh, D. (1986) *Faraday Discuss.* 81, 179–189.
65. Cevc, G., and Marsh, D. (1987) *Phospholipid Bilayers. Physical Principles and Models*, John Wiley & Sons, New York.
66. Bloom, M., and Thewalt, J. L. (1995) *Mol. Membr. Biol.* 12, 9–13.
67. Cruzeiro-Hansson, L., and Mouritsen, O. G. (1988) *Biochim. Biophys. Acta* 944, 63–72.